Porphyrinoids

Deutsche Ausgabe: DOI: 10.1002/ange.201602683
Internationale Ausgabe: DOI: 10.1002/anie.201602683

Spontaneous Formation of an Air-Stable Radical upon the Direct Fusion of Diphenylmethane to a Triarylporphyrin

Kenichi Kato, Wonhee Cha, Juwon Oh, Ko Furukawa, Hideki Yorimitsu,* Dongho Kim,* and Atsuhiro Osuka**

Abstract: *The direct fusion of a diphenylmethane segment to a Ni^{II} 5,10,15-triarylporphyrin with three linkages furnished an air- and moisture-stable neutral radical through unexpected and spontaneous oxidation. This radical was demetalated by treatment with H_2SO_4 and CF_3CO_2H to provide the corresponding free-base radical. These porphyrin radicals are very stable owing to spin delocalization and have been fully characterized through UV/Vis/NIR absorption spectroscopy, X-ray crystallographic analysis, magnetic susceptibility measurements, electrochemical studies, laser-based ultrafast spectroscopic studies, and theoretical calculations. They were chemically oxidized and reduced to the corresponding cation and anion but did not react with hydrogen-atom donors.*

Stable organic radicals have emerged as a promising class of functional molecules.[1] Organic radicals exhibit characteristic electrochemical, optical, and magnetic properties derived from an unpaired electron, which encourages their use in the fields of molecular conductors,[2] spin-based batteries,[3] magnetic bistable materials,[4] and bioimaging.[5] Organic radicals are usually highly reactive and have generally been stabilized by spin delocalization and/or steric protection. In recent years, it has been demonstrated that porphyrinoids are effective platforms to stabilize radicals owing to extensive spin delocalization.[6]

During our studies on π-expanded fused porphyrins, we have explored heteroatom-embedded Ni^{II} porphyrins, such as **1Ni** (nitrogen-embedded),[7] **2Ni** (boron-embedded),[8] and **3Ni** (silicon-embedded)[9] (Scheme 1). These doubly fused porphyrins display intriguing optical and electrochemical properties that arise from the effective interaction of the embedded heteroatom with the porphyrinic π-electronic network in an enforced coplanar conformation. These results encouraged us to attempt the synthesis of fused porphyrin **4Ni**, in which an sp^3-hybridized carbon atom is embedded instead of a heteroatom in the same fused porphyrin structure. Herein, we disclose our attempted synthesis of **4Ni** through the fusion of a diphenylmethane segment directly onto the Ni^{II} porphyrin periphery. Instead we observed the unexpected production of a very stable radical that could be formed by removal of the $C(sp^3)$-bonded hydrogen atom from a putative doubly diphenylmethane fused porphyrin.

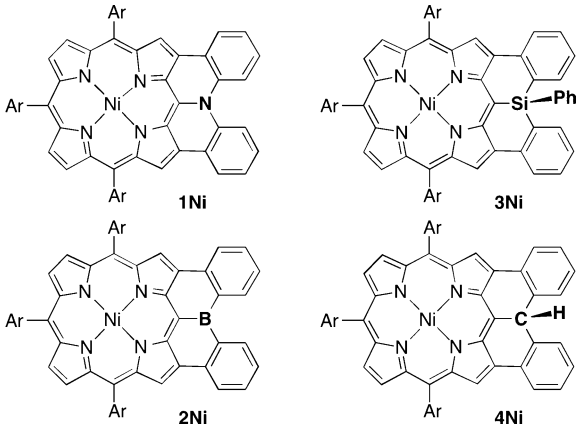

Scheme 1. Heteroatom- and carbon-embedded porphyrins. Ar = 3,5-di-*tert*-butylphenyl.

A two-step reaction sequence was used for the direct fusion of a diphenylmethane segment to the Ni^{II} porphyrin periphery. Following an S_NAr reaction of the Ni^{II} 2,18,20-trichloro-5,10,15-triarylporphyrin **5Ni**[7b] with diphenylmethyllithium to give **6Ni** in 65% yield, we carried out a twofold palladium-catalyzed intramolecular C–H arylation of **6Ni** (Scheme 2). After purification by column chromatography on silica gel and recrystallization from a mixture of CH_2Cl_2 and methanol, a green product was obtained. This product showed a high-resolution (HR) MS (APCI-TOF) peak at m/z 1091.5510 (m/z calcd for $[C_{75}H_{77}N_4{}^{58}Ni]^-$: 1091.5507 [**4Ni**-H]$^-$), thus suggesting a doubly fused structure with one hydrogen atom missing. Intriguingly, the ^1H NMR spectrum of this product was silent except for a broad peak around 1.55 ppm due to the *tert*-butyl groups (see Figure S3-3 in the Supporting Information), and the ESR spectrum exhibited a signal at $g = 2.0007$ (Figure 2a).[10] These results, as well as the X-ray crystal structure (Figure 1), helped us to assign this compound as the neutral porphyrin radical **7Ni**. This assignment suggested that a putative diphenylmethane adduct, **4Ni**, spontaneously released a hydrogen atom to

[*] K. Kato, Prof. Dr. H. Yorimitsu, Prof. Dr. A. Osuka
Department of Chemistry, Graduate School of Science
Kyoto University
Sakyo-ku Kyoto, 606-8502 (Japan)
E-mail: yori@kuchem.kyoto-u.ac.jp
osuka@kuchem.kyoto-u.ac.jp
Prof. Dr. K. Furukawa
Center for Instrumental Analysis, Niigata University
Nishi-ku, Niigata 950-2181 (Japan)
E-mail: kou-f@chem.sc.niigata-u.ac.jp
W. Cha, J. Oh, Prof. Dr. D. Kim
Spectroscopy Laboratory of Functional π-Electronic Systems and
Department of Chemistry, Yonsei University
Seoul 120-749 (Korea)
E-mail: dongho@yonsei.ac.kr

Supporting information for this article can be found under: http://dx.doi.org/10.1002/anie.201602683.

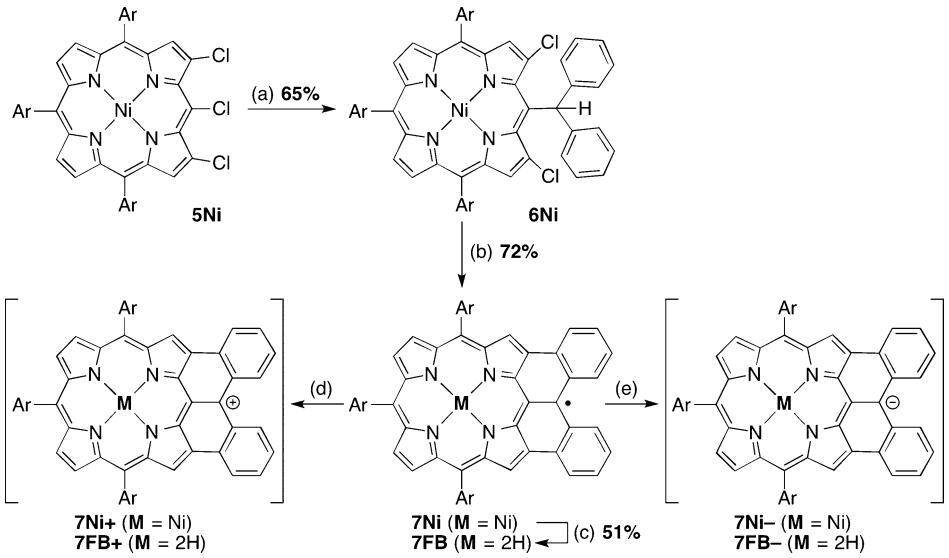

Scheme 2. Synthesis of diphenylmethane-fused porphyrins. Reagents and conditions: a) Ph_2CHLi (2.0 equiv), THF, −98 °C→RT, 2 h; b) $Pd(OAc)_2$ (20 mol%), $PCy_3{\cdot}HBF_4$ (40 mol%), K_2CO_3 (5.0 equiv), toluene, reflux, overnight; c) H_2SO_4/CF_3CO_2H, 0 °C→RT, 45 min; d) $(4\text{-}BrC_6H_4)_3NSbCl_6$, $CDCl_3$, room temperature; e) cobaltocene, $[D_8]$THF, room temperature. Ar = 3,5-di-*tert*-butylphenyl.

generate **7Ni**. In line with this hypothesis, the radical **7Ni** was amazingly stable under ambient conditions: It remained unchanged in solution for at least a month. We attempted to convert **7Ni** into **4Ni** by reaction with hydrogen-atom donors. However, the treatment of **7Ni** with nBu$_3$SnH or ascorbic acid did not cause any change.

The radical character of **7Ni** survived even during demetalation with H_2SO_4/CF_3CO_2H to provide the corresponding free-base radical **7FB**. The HRMS (APCI-TOF), ^{1}H NMR, and ESR spectra and X-ray crystal structure of **7FB** are fully consistent with the proposed structure.

The structures of **7Ni** and **7FB** were revealed unambiguously by X-ray crystallographic analysis to be fairly planar, except for the diphenylmethane moieties, which show a nonplanar [4]helicene-like twist (Figure 1). Two independent molecules were found in both crystals. These molecules form independent antiparallel π-stacked dimers with interplanar distances of 3.51 and 3.56 Å for **7Ni** and 3.56 and 3.61 Å for **7FB**, and offset distances of 3.4–3.5 Å.[11]

The average bond lengths around the radical centers are 1.432(7) Å for C(*meso*)–C(center) and 1.460(7) Å for C(center)–C(phenyl *ipso*) in **7Ni** and 1.429(5) Å for C(*meso*)–C(center) and 1.460(5) Å for C(center)–C(phenyl *ipso*) in **7FB**. The sum of the three angles around the radical centers is 360.0° in each case. These structural data indicate perfect sp^2 hybridization for the radical center. The bond lengths of the porphyrin segments are almost unchanged as compared to those of the non-substituted triarylporphyrins (see Figure S7-4).

Figure 2c shows the UV/Vis/NIR absorption spectra of **7Ni** and **7FB**. The absorption spectrum of **7Ni** is composed of a relatively weak Soret-like band (481 nm) and Q-like bands (582 and 620 nm), along with several weak and broad bands up to 1500 nm. Similarly, that of **7FB** shows a broadened Soret-like band at 475 nm, Q-like bands at 564 and 633 nm, and weak and broad bands up to 1500 nm. The observed low-energy broad absorption bands are characteristic of porphyr-

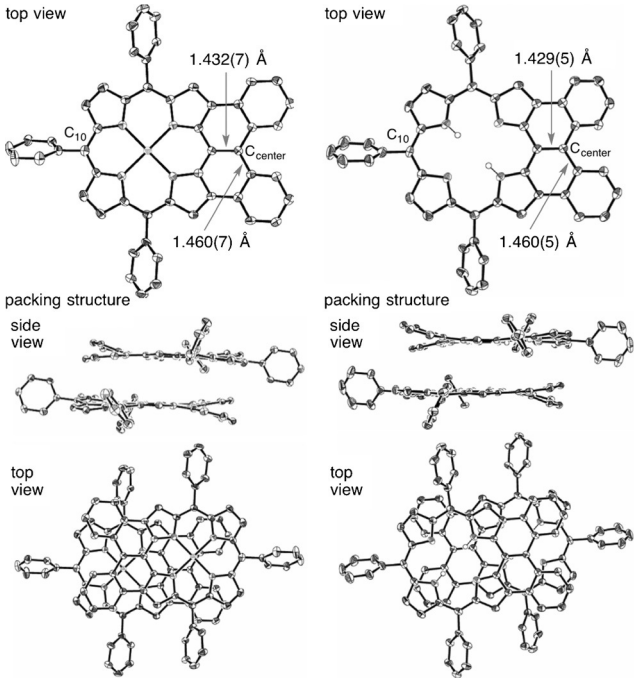

Figure 1. X-ray crystal structures of **7Ni** (left) and **7FB** (right). One of two independent molecules is shown in each view at 50% thermal-ellipsoid probability. Solvent molecules, *tert*-butyl groups, and hydrogen atoms, except for NH groups, are omitted for clarity.

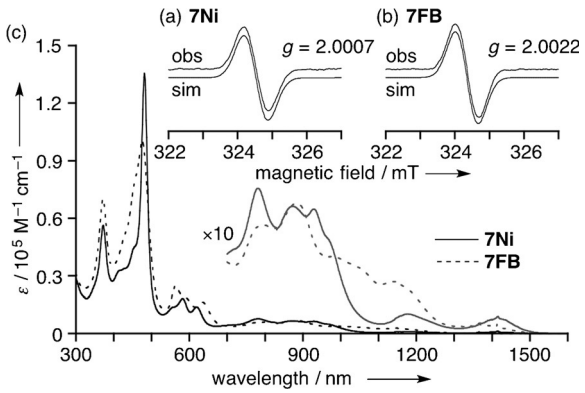

Figure 2. Observed and simulated X-band ESR spectra of a) **7Ni** and b) **7FB** in toluene (5.9×10^{-5} and 5.4×10^{-5} M solution, respectively) at room temperature. The spectral simulation was performed with the Easyspin program package.[14] c) UV/Vis/NIR absorption spectra of **7Ni** (solid line) and **7FB** (dashed line) in CH_2Cl_2.

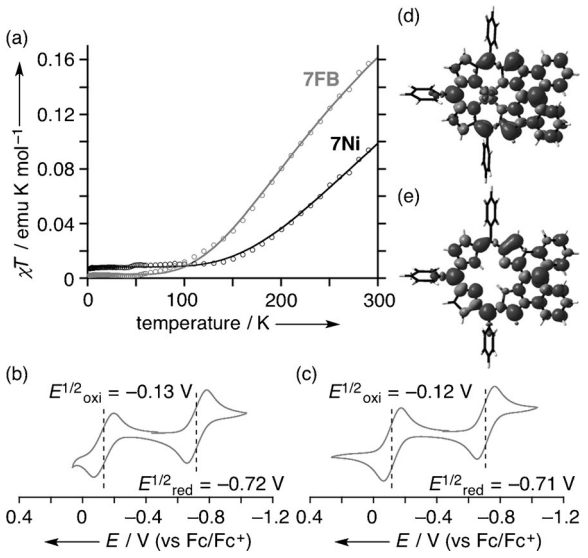

Figure 3. a) Observed (circles) and simulated (lines) χT values of **7Ni** (black) and **7FB** (gray). Applied field: 0.5 T. b, c) Cyclic voltammograms of **7Ni** (b) and **7FB** (c) in CH_2Cl_2 containing 0.1 M nBu_4NPF_6 as a supporting electrolyte. Scan rate: 0.05 Vs^{-1}; working electrode: Pt; counter electrode: Pt wire; reference electrode: $Ag/AgClO_4$. Ferrocene/ferrocenium cation was used as an external reference. d, e) Spin-density-distribution plots of **7Ni** (d) and **7FB** (e) as calculated at the UB3LYP/6-31G(d) level (isovalue: 0.001).

inoid radicals.[6] Time-dependent DFT calculations at the UB3LYP/6-31G(d) level[12] predicted that the lowest-energy transitions of **7Ni** and **7FB** are HOMO–SOMO transitions.[13]

The magnetic properties in the solid state were examined by temperature-dependent magnetic susceptibility measurements (SQUID; Figure 3a). The observed χT plots were appropriately reproduced with the Bleaney–Bowers singlet–triplet model[15] [Eq. (1) and (2)] with fit parameters (f_1, f_2, J_1/k_B, J_1) = (1.00, 0.011, −391 K, −272 cm^{-1}) for **7Ni** and (1.00, 0.004, −279 K, −194 cm^{-1}) for **7FB**. Although we used powder samples of **7Ni** and **7FB** for the SQUID study, they were thought to assemble in a similar manner to their single crystals on a microscopic scale.[16] These radicals exhibited a relatively strong antiferromagnetic interaction due to their π-stacked structures. We interpret the different antiferromagnetic interactions of **7Ni** and **7FB** in terms of different interplanar distances.

$$H = -2J_1 s_a s_b + \mu_B \sum_{i=a,b} s_i g_i H_{ex} \quad (1)$$

$$\chi T = f_1 \frac{N_A g^2 {\mu_B}^2}{k_B[3 + \exp(-2J_1/k_B T)]} + f_2 \frac{N_A g^2 {\mu_B}^2}{2k_B} \quad (2)$$

The electrochemical properties of **7Ni** and **7FB** were also investigated by cyclic voltammetry in CH_2Cl_2 (Figure 3b,c). Each radical showed fairly reversible oxidation and reduction waves with a narrow electrochemical gap (0.59 eV for both radicals). Spin-density distributions calculated at the UB3LYP/6-31G(d) level[12] also show extensive spin delocalization over the whole fused π-network (Figure 3d,e), as attributed to the rigidly held planar structures with perpendicular p orbitals. Similar spin delocalization was reported for other planar organic radicals,[17] which were not as stable as **7Ni** and **7FB**, thus underlining the effective radical-stabilization ability of porphyrins.

To gain further insight into the radical nature of **7Ni** and **7FB**, we explored their excited-state dynamics by femtosecond transient absorption (TA) measurements. The TA spectra of **7Ni** and **7FB** rapidly decayed with two time constants of 0.5 and 8 ps for **7Ni**, and 0.3 and 9 ps for **7FB** (see Figure S11-1). These two decay components are ascribed to an internal conversion process to the lowest excited state and relaxation to the open-shell ground state, respectively, in good accordance with a high density of states in **7Ni** and **7FB** owing to their radical character.[6a,d] Furthermore, we conducted two-photon absorption (TPA) measurements by using an open-aperture Z-scan method for **7Ni** and **7FB**. The maximum TPA cross-section value was 630 and 580 GM at 1500 nm for **7Ni** and **7FB**, respectively (see Figures S12-1 and S12-2). The significantly enhanced TPA values of **7Ni** and **7FB** as compared to very low TPA cross-section values of typical porphyrinoids (< 100 GM) are ascribed to their stable spin-delocalized π-radical character.[6b,18]

The highly reversible redox behavior of the radicals prompted us to attempt the chemical oxidation and reduction of **7Ni**. A titration with tris(4-bromophenyl)aminium hexachloroantimonate led to smooth spectral changes with the emergence of new bands to indicate the generation of the corresponding cationic species **7Ni+** (see Figure S6-4). The resultant solution displayed a symmetric ^1H NMR spectrum featuring signals due to the pyrrolic β-hydrogen atoms at 5.96, 5.86, and 5.74 ppm (see Figure S3-11), which are shifted upfield considerably as compared to those of usual porphyrins (ca. 9.0–8.5 ppm), thus suggesting significant electronic perturbation of the porphyrinic electron network. Similarly, a titration with cobaltocene caused smooth spectral changes (see Figure S6-5) indicating the generation of the corresponding anionic species **7Ni−**. As compared with **7Ni+**, the ^1H NMR of **7Ni−** was less perturbed, since it showed signals due to the pyrrolic β-hydrogen atoms at 8.66, 7.92, and 7.70 ppm (see Figure S3-11). These contrasting spectral features of **7Ni+** and **7Ni−** may be accounted for in terms of effective resonance hybrids (see Figure S3-11). Besides the 18π electronic resonance hybrid, antiaromatic 20π and 24π resonance hybrids may contribute to the electronic network of **7Ni+**, whereas aromatic 22π and 26π resonance hybrids may contribute to the electronic network of **7Ni−**. This interpretation is supported by nucleus-independent chemical shift (NICS) values[19] (see Table S10-1) and anisotropy-induced current density (ACID) plots[20] calculated at the B3LYP/6-31G(d) level (see Figure S10-5). The cation **7Ni+** shows a counterclockwise induced ring current on 20-membered circuit with positive NICS(0) values (+4.45 to +12.6 ppm) inside the circuit. On the other hand, for **7Ni−**, a clockwise induced ring current on the outermost 30-membered circuit was observed in the ACID plot, and negative NICS(0) values (−5.78 to −13.6 ppm) were estimated.

The UV/Vis/NIR absorption spectra of **7Ni+** and **7Ni−** display Soret-like bands at 516 and 477 nm and Q-like bands

at 743 and 829 nm, respectively, with broad and weak NIR absorption bands above 1000 nm (see Figures S6-4 and S6-5). The TA spectra of **7Ni+** and **7Ni**− show biexponential decay dynamics fitted with time constants of 0.8 and 12 ps and 0.9 and 35 ps, respectively (see Figure S11-1). Notably, **7Ni**− has a longer S_1 state lifetime than that of **7Ni+**. Typically, aromatic porphyrinoids exhibit a slow deactivation process as compared to the rapid decay of antiaromatic porphyrinoids.[21] Thus, along with the ^{1}H NMR spectroscopic results for **7Ni+** and **7Ni**−, these different decay dynamics are attributable to their antiaromatic and aromatic nature, respectively.

In summary, an air-stable radical **7Ni** was formed upon the direct fusion of a diphenylmethane segment to a 5,10,15-triaryl Ni^{II} porphyrin, and its demetalation provided **7FB**. These radicals are extremely stable owing to extensive spin delocalization over the porphyrin π-electronic network. These radicals formed antiparallel π-stacked dimers with a relatively strong antiferromagnetic interaction in the solid state. They underwent highly reversible electrochemical one-electron oxidation and reduction, and the chemical oxidation and reduction of **7Ni** provided the cation **7Ni+** and anion **7Ni**−, whose ^{1}H NMR spectra were rationalized by considering expanded macrocyclic electron circuits in addition to the 18π porphyrinic network. Further elaboration of these stable radicals is ongoing in our laboratories.

Acknowledgements

The research at Kyoto was supported by Grants-in-Aid from MEXT (No.: 25107002 "Science of Atomic Layers") and from JSPS (No.: 25220802 (Scientific Research (S)), 24685007 (Young Scientists (A)), and 26620081 (Exploratory Research)), and by ACT-C, JST. We thank Prof. Dr. Hiroshi Kitagawa and Dr. Kazuya Otsubo (Kyoto University) for XRPD measurements. H.Y. thanks Kansai Research Foundation for Technology Promotion and The Asahi Glass Foundation for financial support. The research at Yonsei University was supported by the Ministry of Science, ICT & Future, Korea through the Global Research Laboratory Program (2013K1A1A2A02050183).

Keywords: aromaticity · fused-ring systems · porphyrinoids · radical · redox chemistry

How to cite: *Angew. Chem. Int. Ed.* **2016**, *55*, 8711–8714
Angew. Chem. **2016**, *128*, 8853–8856

[1] a) *Stable Radicals*: *Fundamentals and Applied Aspects of Odd-Electron Compounds* (Ed.: R. D. Hicks), Wiley-Blackwell, New York, **2010**; b) R. D. Hicks, *Org. Biomol. Chem.* **2007**, *5*, 1321.
[2] S. K. Mandal, S. Samanta, M. E. Itkis, D. W. Jensen, R. W. Reed, R. T. Oakley, F. S. Tham, B. Donnadieu, R. C. Haddon, *J. Am. Chem. Soc.* **2006**, *128*, 1982.
[3] Y. Morita, S. Nishida, T. Murata, M. Moriguchi, A. Ueda, M. Satoh, K. Arifuku, K. Sato, T. Takui, *Nat. Mater.* **2011**, *10*, 947.
[4] a) R. G. Hicks, *Nat. Chem.* **2011**, *3*, 189; b) M. E. Itkis, X. Chi, A. W. Cordes, R. C. Haddon, *Science* **2002**, *296*, 1443.
[5] A. Rajca, Y. Wang, M. Boska, J. T. Peletta, A. Olankitwanit, M. A. Swanson, D. G. Mitchell, S. S. Eaton, G. R. Eaton, S. Rajca, *J. Am. Chem. Soc.* **2012**, *134*, 15724.
[6] For stable porphyrinoid radicals, see: a) T. Koide, G. Kashiwazaki, M. Suzuki, K. Furukawa, M.-C. Yoon, S. Cho, D. Kim, A. Osuka, *Angew. Chem. Int. Ed.* **2008**, *47*, 9661; *Angew. Chem.* **2008**, *120*, 9807; b) M. Ishida, J.-Y. Shin, J.-M. Lim, B. S. Lee, M.-C. Yoon, T. Koide, J. L. Sessler, A. Osuka, D. Kim, *J. Am. Chem. Soc.* **2011**, *133*, 15533; c) T. Y. Gopalakrishna, J. S. Reddy, V. G. Anand, *Angew. Chem. Int. Ed.* **2014**, *53*, 10984; *Angew. Chem.* **2014**, *126*, 11164; d) D. Shimizu, J. Oh, K. Furukawa, D. Kim, A. Osuka, *Angew. Chem. Int. Ed.* **2015**, *54*, 6613; *Angew. Chem.* **2015**, *127*, 6713; e) P. Schweyen, K. Brandhorst, R. Wicht, B. Wolfram, M. Bröring, *Angew. Chem. Int. Ed.* **2015**, *54*, 8213; *Angew. Chem.* **2015**, *127*, 8331; f) D. Shimizu, J. Oh, K. Furukawa, D. Kim, A. Osuka, *J. Am. Chem. Soc.* **2015**, *137*, 15584; g) L. J. Esdaile, L. Rintoul, M. S. Goh, K. Merahi, N. Parizel, R. M. Wellard, S. Choua, D. P. Arnold, *Chem. Eur. J.* **2016**, *22*, 3430.
[7] a) N. Fukui, W.-Y. Cha, S. Lee, S. Tokuji, D. Kim, H. Yorimitsu, A. Osuka, *Angew. Chem. Int. Ed.* **2013**, *52*, 9728; *Angew. Chem.* **2013**, *125*, 9910; b) N. Fukui, H. Yorimitsu, A. Osuka, *Angew. Chem. Int. Ed.* **2015**, *54*, 6311; *Angew. Chem.* **2015**, *127*, 6409.
[8] K. Fujimoto, J. Oh, H. Yorimitsu, D. Kim, A. Osuka, *Angew. Chem. Int. Ed.* **2016**, *55*, 3196; *Angew. Chem.* **2016**, *128*, 3248.
[9] K. Kato, J. O. Kim, H. Yorimitsu, D. Kim, A. Osuka, *Chem. Asian J.*, DOI: 10.1002/asia.201600424.
[10] The g value was smaller than for a free electron ($g = 2.0023$) owing to spin–orbital interaction with the nickel atom.
[11] The interplanar distances were calculated for the mean planes of 24 porphyrinic and 13 diphenylmethyl atoms. The center of the plane is defined as the midpoint between C_{center} and C_{10} atoms.
[12] a) Gaussian 09 (Revision A.02), M. J. Frisch, et al. Gaussian, Inc. Wallingford CT, **2009**; b) A. D. Becke, *J. Chem. Phys.* **1993**, *98*, 1372; c) C. Lee, W. Yang, R. G. Parr, *Phys. Rev. B* **1988**, *37*, 785.
[13] The oscillator strength was calculated to be $f = 0.0030$ (1138 nm) for **7Ni** and $f = 0.0043$ (1102 nm) for **7FB**. For further information, see Figures S6-2 and S6-3.
[14] S. Stoll, A. Schweiger, *J. Magn. Reson.* **2006**, *178*, 42.
[15] B. Bleaney, K. D. Bowers, *Proc. R. Soc. London, Ser. A* **1952**, *214*, 451.
[16] The PXRD patterns of the radicals were similar to those simulated for the crystals (see Figure S7-5).
[17] a) E. Müller, A. Moosmayer, A. Rieker, K. Scheffler, *Tetrahedron Lett.* **1967**, *8*, 3877; b) D. Hellwinkel, M. Melan, G. Aulmich, *Tetrahedron Lett.* **1976**, *17*, 4137; c) F. A. Neugebauer, D. Hellwinkel, G. Aulmich, *Tetrahedron Lett.* **1978**, *19*, 4871.
[18] a) M. Nakano, R. Kishi, T. Nitta, T. Kubo, K. Nakasuji, K. Kamada, K. Ohta, B. Champagne, E. Botek, K. Yamaguchi, *J. Phys. Chem. A* **2005**, *109*, 885; b) Y. Hisamune, K. Nishimura, K. Isakari, M. Ishida, S. Mori, S. Karasawa, T. Kato, S. Lee, D. Kim, H. Furuta, *Angew. Chem. Int. Ed.* **2015**, *54*, 7323; *Angew. Chem.* **2015**, *127*, 7431.
[19] a) P. von R. Schleyer, C. Maerker, A. Dransfeld, H. Jiao, N. J. R. van Eikema Hommes, *J. Am. Chem. Soc.* **1996**, *118*, 6317; b) Z. Chen, C. S. Wannere, C. Corminboeuf, R. Puchta, P. von R. Schleyer, *Chem. Rev.* **2005**, *105*, 3842.
[20] R. Herges, D. Geuenich, *J. Phys. Chem. A* **2001**, *105*, 3214.
[21] J.-Y. Shin, K. S. Kim, M.-C. Yoon, J. M. Lim, Z. S. Yoon, A. Osuka, D. Kim, *Chem. Soc. Rev.* **2010**, *39*, 2751.

Received: March 17, 2016
Published online: June 3, 2016

